npj | Quantum Information

www.nature.com/npjqi

ARTICLE OPEN

Efficient quantum simulation of photosynthetic light harvesting

Bi-Xue Wang[1], Ming-Jie Tao[1,2], Qing Ai[2,3], Tao Xin[1], Neill Lambert[3], Dong Ruan[1], Yuan-Chung Cheng[4], Franco Nori[3,5], Fu-Guo Deng[2,6] and Gui-Lu Long[1,7,8,9,10]

Near-unity energy transfer efficiency has been widely observed in natural photosynthetic complexes. This phenomenon has attracted broad interest from different fields, such as physics, biology, chemistry, and material science, as it may offer valuable insights into efficient solar-energy harvesting. Recently, quantum coherent effects have been discovered in photosynthetic light harvesting, and their potential role on energy transfer has seen the heated debate. Here, we perform an experimental quantum simulation of photosynthetic energy transfer using nuclear magnetic resonance (NMR). We show that an *N*-chromophore photosynthetic complex, with arbitrary structure and bath spectral density, can be effectively simulated by a system with $\log_2 N$ qubits. The computational cost of simulating such a system with a theoretical tool, like the hierarchical equation of motion, which is exponential in *N*, can be potentially reduced to requiring a just polynomial number of qubits *N* using NMR quantum simulation. The benefits of performing such quantum simulation in NMR are even greater when the spectral density is complex, as in natural photosynthetic complexes. These findings may shed light on quantum coherence in energy transfer and help to provide design principles for efficient artificial light harvesting.

npj Quantum Information (2018)4:52 ; doi:10.1038/s41534-018-0102-2

INTRODUCTION

Efficient exciton energy transfer (EET) is crucial in photosynthesis and solar cells,[1,2] especially when the systems are large,[3] e.g., as in Photosystem I (PSI) and Photosystem II (PSII), which have hundreds of chromophores. A comprehensive knowledge of the quantum dynamics of such systems would be of potential importance to the study on EET.[4] Much effort has been made to reveal the effects of quantum coherence on efficient energy transfer.[4–11] In order to try to mimic EET, a Frenkel-exciton Hamiltonian is required and this can be studied with quantum chemistry approaches,[1] e.g., fitting experimental spectra, or calculations by density functional theory. Because photosynthetic pigment–protein complexes are intrinsically open quantum systems, with system-bath couplings comparable to the intra-system couplings, it is difficult to faithfully mimic the exact quantum dynamics of EET. Among the methods for describing EET,[1,11–13] the hierarchical equation of motion (HEOM) yields a numerically exact solution at the cost of considerable computing time.[11,14] For the widely-studied Fenna–Matthews–Olson (FMO) complex,[5,6,11,13,15,16] a reliable result could be produced by 16,170 coupled differential equations at low temperatures, based on the HEOM[11,14] with 4 layers. Moreover, the HEOM encounters difficulties when the system has non-trivial spectral density, making it often difficult to verify the results. On the other hand, due to heterogeneity, e.g., static disorder and conformational change, it is difficult to experimentally verify the theoretical predictions in natural photosynthetic systems. Because quantum simulations with *N* qubits can powerfully mimic the quantum dynamics of 2^N states by virtue of quantum mechanics,[17–19] the quantum simulation of photosynthetic energy transfer with an arbitrary Hamiltonian by nuclear magnetic resonance (NMR) provides an intriguing approach to verify theoretical predictions. Recently, a newly-developed technique which could simulate the effect of a bath with an arbitrary spectral density by a set of classical pulses has been successfully realized with ion traps[20] and NMR.[21] Therefore, photosynthetic light-harvesting with an arbitrary Hamiltonian and spectral density, describing a structured environment, can be experimentally simulated by NMR.

RESULTS

NMR is an excellent platform for quantum simulation since it is easy to operate and it can have long coherence times.[22,23] In this paper, NMR is utilized to simulate the quantum coherent dynamics in photosynthetic light harvesting. As a prototype, a tetramer including four chlorophylls,[13] as schematically illustrated in Fig. 1a, is employed in the NMR quantum simulation. In a previous investigation,[13] the tetramer model was exploited to study the clustered geometry utilizing exciton delocalization and energy matching to accelerate the energy transfer. The EET in

[1]State Key Lab for Low-dimensional Quantum Physics, Department of Physics, Tsinghua University, Beijing 100084, China; [2]Department of Physics, Applied Optics Beijing Area Major Laboratory, Beijing Normal University, Beijing 100875, China; [3]Theoretical Quantum Physics Laboratory, RIKEN Cluster for Pioneering Research, Wako-shi, Saitama 351-0198, Japan; [4]Department of Chemistry, National Taiwan University, Taipei City 106, Taiwan; [5]Physics Department, The University of Michigan, Ann Arbor, MI 48109-1040, USA; [6]NAAM-Research Group, Department of Mathematics, Faculty of Science, King Abdulaziz University, Jeddah 21589, Saudi Arabia; [7]Beijing National Research Center on Information Science and Technology, Beijing 100084, China; [8]School of Information Science and Technology, Tsinghua University, Beijing 100084, China; [9]Innovation Center of Quantum Matter, Beijing 100084, China and [10]Beijing Academy of Quantum Information, Beijing 100085, China
Correspondence: F-G. Deng (fgdeng@bnu.edu.cn) or G-L. Long (gllong@tsinghua.edu.cn)
These authors contributed equally: Bi-Xue Wang, Ming-Jie Tao, Qing Ai.

Received: 15 March 2018 Revised: 10 August 2018 Accepted: 24 September 2018
Published online: 22 October 2018

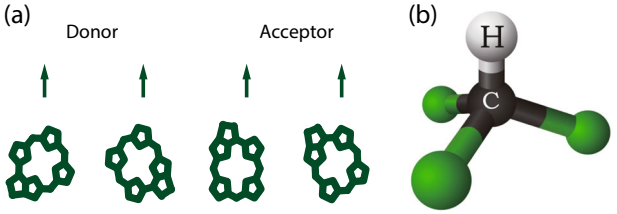

Fig. 1 Photosynthetic chromophore arrangement and physical system for NMR simulation. **a** Linear geometry with four chromophores for photosynthetic energy transfer. **b** Chemical structure for a ^{13}C-labeled chloroform molecule, where the H and C nuclear spins are chosen as the two qubits

photosynthesis is described by the Frenkel-exciton Hamiltonian

$$H_{\mathrm{EET}} = \sum_{i=1}^{4} \varepsilon_i |i\rangle\langle i| + \sum_{i\neq j=1}^{4} J_{ij} |i\rangle\langle j|, \tag{1}$$

where $|i\rangle$ ($i = 1, 2, 3, 4$) is the state with a single excitation at site i and other sites at the ground state, ε_i is the site energy of $|i\rangle$, J_{ij} is the excitonic interaction between sites i and j. In our quantum simulations, we adopt the site energies[13] $\varepsilon_1 = 13{,}000\ \mathrm{cm}^{-1}$, $\varepsilon_2 = 12{,}900\ \mathrm{cm}^{-1}$, $\varepsilon_3 = 12{,}300\ \mathrm{cm}^{-1}$, and $\varepsilon_4 = 12{,}200\ \mathrm{cm}^{-1}$, and the couplings $J_{12} = J_{34} = 126\ \mathrm{cm}^{-1}$, $J_{13} = J_{24} = 16\ \mathrm{cm}^{-1}$, $J_{23} = 132\ \mathrm{cm}^{-1}$, and $J_{14} = 5\ \mathrm{cm}^{-1}$, which are typical parameters in photosynthetic systems.

For a photosynthetic complex with N chlorophylls, there are only N single-excitation states involved in the energy transfer. Therefore, only $\log_2 N$ qubits are required to realize the quantum simulation. To mimic the energy transfer described by the above Hamiltonian (1), two qubits are necessary for the quantum simulation. In this case, the photosynthetic single-excitation state $|i\rangle$ is encoded as a two-qubit product state, i.e., $|00\rangle$, $|01\rangle$, $|10\rangle$, and $|11\rangle$. By a straightforward calculation, the Frenkel-exciton Hamiltonian can be mapped to the NMR Hamiltonian as

$$\begin{aligned} H_{\mathrm{NMR}} = {} & \tfrac{\varepsilon_1'+\varepsilon_2'-\varepsilon_3'-\varepsilon_4'}{4}\sigma_1^z + \tfrac{\varepsilon_1'-\varepsilon_2'+\varepsilon_3'-\varepsilon_4'}{4}\sigma_2^z \\ & + \tfrac{J_{13}'+J_{24}'}{2}\sigma_1^x + \tfrac{J_{12}'+J_{34}'}{2}\sigma_2^x + \tfrac{J_{14}'+J_{23}'}{2}\sigma_1^x\sigma_2^x \\ & + \tfrac{J_{23}'-J_{14}'}{2}\sigma_1^y\sigma_2^y + \tfrac{J_{13}'-J_{24}'}{2}\sigma_1^x\sigma_2^z \\ & + \tfrac{J_{12}'-J_{34}'}{2}\sigma_1^z\sigma_2^x, \end{aligned} \tag{2}$$

where σ_j^u ($j = 1, 2$, $u = x, y, z$) is the Pauli operator for qubit j, numerically $\varepsilon_j' = \pi\varepsilon_j/10$ and $J_{ij}' = \pi J_{ij}/10$, but the dimension cm^{-1} should be replaced by kHz. In other words, all realistic parameters have been scaled down in energy by a factor of $1\ \mathrm{cm}^{-1}/(\pi/10\ \mathrm{kHz}) = 3\times10^8/\pi$.

The excitonic coupling J_{ij} between sites i and j makes the exciton energy hop in both directions, i.e., $|i\rangle \leftrightarrows |j\rangle$. Apart from this, the system-bath couplings will facilitate the energy flow towards an energy trap, where the captured photon energy is converted into chemical energy.[2,3] The interaction between the system and bath in photosynthetic complexes can be described by

$$H_{\mathrm{SB}} = \sum_{i,k} g_{ik} |i\rangle\langle i| \left(a_{ik}^{\dagger} + a_{ik}\right), \tag{3}$$

where $a_{ik}^{\dagger}$ is the creation operator for the kth phonon mode of chlorophyll i with coupling strength g_{ik}. H_{SB} will induce pure-dephasing on the i-th chromophore when it is in the excited state. Generally, the system-bath couplings are given by the spectral density

$$G_{\mathrm{EET}}(\omega) = \sum_{k} g_{ik}^2 \delta(\omega - \omega_k), \tag{4}$$

which we assume identical for all chromophores. For typical photosynthetic complexes, the system-bath couplings are of the same order as the intra-system couplings. In order to mimic the effects of noise, we utilize the bath-engineering technique which has been successfully implemented in ion traps and NMR. The implementation of a pure-dephasing Hamiltonian

$$H_{\mathrm{PDN}} = \vec{B}(t)\cdot\vec{\sigma} \tag{5}$$

relies on generating stochastic errors by performing phase modulations on a constant-amplitude carrier, i.e.,

$$\vec{B}(t) = \Omega_0 \cos\left[\omega_\mu t + \phi_N(t)\right]\hat{z}, \tag{6}$$

$$\phi_N(t) = \alpha \sum_{j=1}^{J} F(j) \sin\left(\omega_j t + \psi_j\right), \tag{7}$$

where Ω_0 is the constant amplitude of a magnetic field with driving frequency ω_μ, ψ_j is a random number, $\omega_j = j\omega_0$ with ω_0 and $\omega_J = J\omega_0$ being base and cutoff frequencies, respectively, and α is a global scaling factor. The power-spectral density $S_z(\omega) \equiv \int d\tau \langle \dot{\phi}_N(t+\tau)\dot{\phi}_N(t)\rangle e^{i\omega\tau}$ is the Fourier transform of the auto-correlation function of $\dot{\phi}_N(t)$,

$$S_z(\omega) = \frac{\pi\alpha^2\omega_0^2}{2} \sum_{j=1}^{J} j^2 F^2(j) \left[\delta\left(\omega-\omega_j\right) + \delta\left(\omega+\omega_j\right)\right]. \tag{8}$$

By appropriately choosing $F(j)$ and the cutoff J, an arbitrary power-spectral density of the bath can be realized, e.g., white, Ohmic, or Drude–Lorentz spectral densities. For the details, please refer to the Supplementary Information.

As illustrated in Fig. 1b, the nuclear spins of the carbon atom and hydrogen atom in a chloroform molecule are chosen to encode the two qubits with the Hamiltonian written as

$$H_{\mathrm{CHCl_3}} = \pi\omega_1\sigma_1^z + \pi\omega_2\sigma_2^z + \frac{\pi J}{2}\sigma_1^z\sigma_2^z, \tag{9}$$

where $\omega_1 = 3206.5$ Hz, $\omega_2 = 7787.9$ Hz are the chemical shifts of the two spins, and $J = 215.1$ Hz (ref. [24]). Therefore, in order to simulate the quantum dynamics of energy transfer, the entire evolution is decomposed into repetitive identical cycles. After each cycle, there is a small difference between the exact evolution and the simulated one. However, because there are tens of thousands of cycles before completing the energy transfer, the accumulated error might be significant so that the simulation becomes unreliable. To avoid this problem, we utilize the gradient ascent pulse engineering (GRAPE) algorithm,[25] which has been successfully applied to a number of quantum simulations in NMR,[23,26,27] to mimic the quantum dynamics of light harvesting.

Before studying the population dynamics, we shall explore the characteristics of the artificially injected noise. Generally, the noise is characterized by Ramsey interference measurements, as shown in Fig. 2. When there is no noise applied to the system, we would expect coherent evolution without damping. However, as the artificial noise is applied, the oscillations become damped. The envelope of the damped oscillations is fully determined by the noise strength. Interestingly, for the parameters employed in this work for a broad-frequency background bath, the NMR experimental results *exactly* fit the theoretical prediction by HEOM. This suggests that our technique for injecting artificial noise can, in this limit, faithfully reproduce the effect of the protein environment on natural photosynthetic complexes.

In Fig. 3a, the quantum coherent energy transfer for the above Hamiltonian $H_{\mathrm{NMR}} + H_{\mathrm{PDN}}$, using an initial condition where an excitation is localized on the first chromophore, is simulated in NMR. In the short-time regime, cf. Fig. 3b, there are Rabi-like oscillations of coherent energy transfer between the two levels with the highest energies, because there is a strong coupling between these two levels. Furthermore, the oscillation quickly damps as the energy transfer is irreversible due to the pure-dephasing noise. After an exponential decay process, the

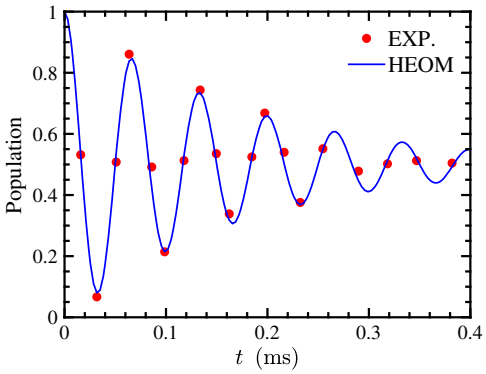

Fig. 2 The decay of the population of the state $|0\rangle$. The theoretical simulation adopting HEOM is shown by the blue curve, and the experimental data by the red dots. In our experiment, the parameters are $\varepsilon_D - \varepsilon_A = 2\pi \times 15$ kHz, $dt = 20$ μs, and $M = 50$. The parameters of the Drude–Lorentz noise are $\gamma_{\mathrm{NMR}} = 2\pi \times 45$ kHz, $\lambda_{\mathrm{NMR}} = 2\pi \times 0.01$ kHz, $T_{\mathrm{EET}} = 300$ K, $\omega_0 = 2\pi \times 5$ Hz, and $\omega_J = 2\pi \times 25$ kHz

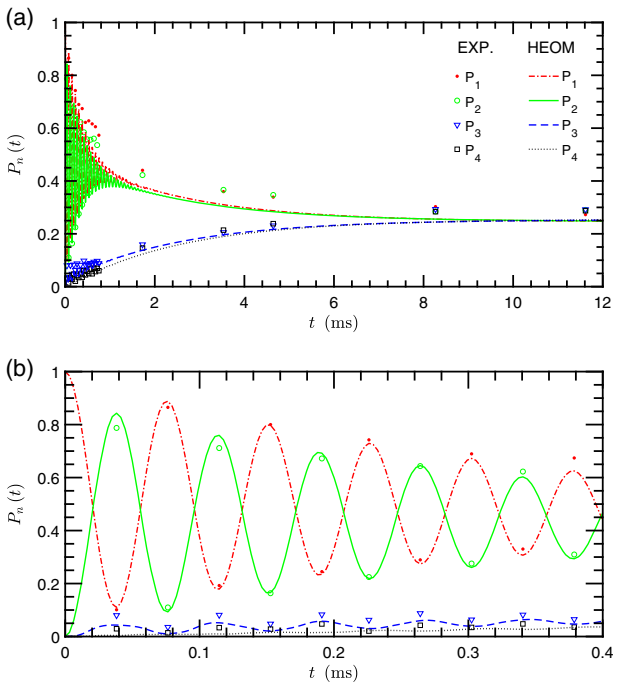

Fig. 3 Simulation of the energy transfer governed by $H_{\mathrm{NMR}} + H_{\mathrm{PDN}}$ for $M = 150$ random realizations. **a** Long-time quantum dynamics; **b** short-time quantum dynamics. The symbols show the experimental data, and the curves are obtained from the numerical simulation using the HEOM. In all figures, the horizontal coordinates of the curves for EET dynamics have been magnified by $3 \times 10^8/\pi$ times

populations on all levels reach thermal equilibrium. Noticeably, there are small oscillations for the two lowest-energy levels as a result of their strong coupling. For each point in the quantum simulation, the data is averaged over M random realizations. For a given realization, the system undergoes a coherent evolution by applying a time-dependent magnetic field with fluctuating phases, as shown in Eqs. (6) and (7). However, for an ensemble of random realizations, since each realization experiences a different phase at a given time, the ensemble average manifests itself as a single realization undergoing a pure-dephasing noise. In this regard, the deviation of the NMR simulation from that predicted by the HEOM decreases as the number of realizations in the ensemble increases. In Fig. 4, we show the effect on the

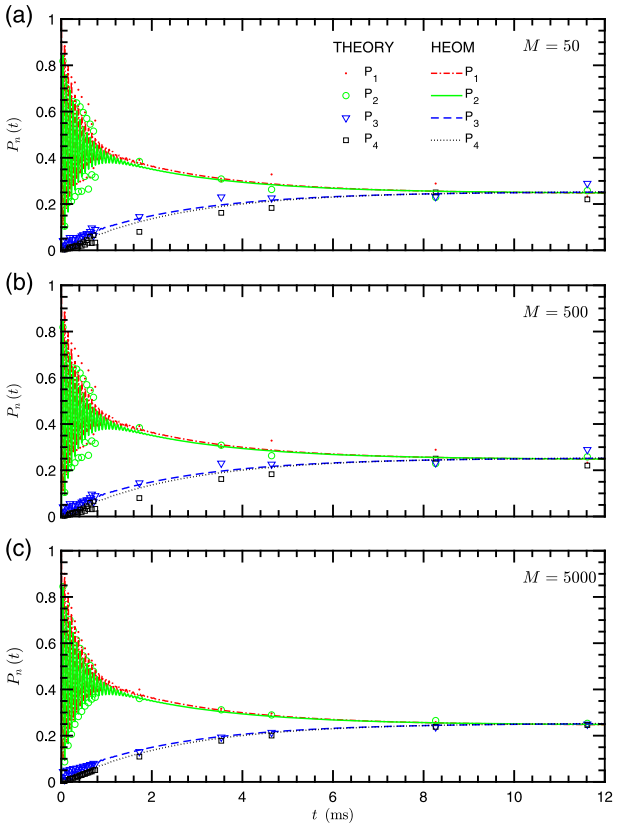

Fig. 4 Effect of the ensemble size on the simulations. The symbols show the theoretical results and the curves show the HEOM results. The number of realizations in each ensemble are $M = 50$ **a**, 500 **b**, and 5000 **c**

simulation error of the number of realizations in each ensemble. Both results, by NMR and by HEOM, converge as M increases, such that the difference between them can hardly be noticed when $M \sim 500$. This effect would be more remarkable if M were increased further, as confirmed by our theoretical simulations in the Supplementary Information. In conclusion, the dephasing Hamiltonian (3) in photosynthesis is effectively mimicked by a classical time-fluctuating magnetic field ((6) and (7)).

It has been suggested in the literature[6,28,29] that the long-lasting electronic coherence observed in experiments might be attributed to strong coupling to vibrational modes. Therefore, it is interesting to consider whether it is possible to simulate some features of underdamped vibrational modes in the NMR platform. In photosynthesis, the coupling to a vibrational mode can be described by $\sum_i g_{iv}|i\rangle\langle i|\left(a_{iv}^{\dagger} + a_{iv}\right)$. In order to simulate the underdamped vibrational mode in our protocol, we can supplement an additional term, i.e., $aF(v)\sin(\omega_v t)$ into Eq. (7). In Fig. 5, we show the numerical simulation for the above 4-level system including such a "semi-classical" vibrational mode. Because we set the vibrational mode to be closely-resonant with the two lower exciton states, there is significantly prolonged coherence in the two lower energy states in the short-time regime, as compared to Fig. 3. Since there is no random phase associated with this modulation, and quantum properties of the vibrational mode are neglected, each realization will evolve uniformly in Fig. 5. Therefore, the long-lasting coherence is driven by the nearly-resonant driving. Going beyond a semi-classical approach, and accurately capturing the quantum features of this mode, requires the use of ancillary degrees of freedom, as discussed in the conclusions.

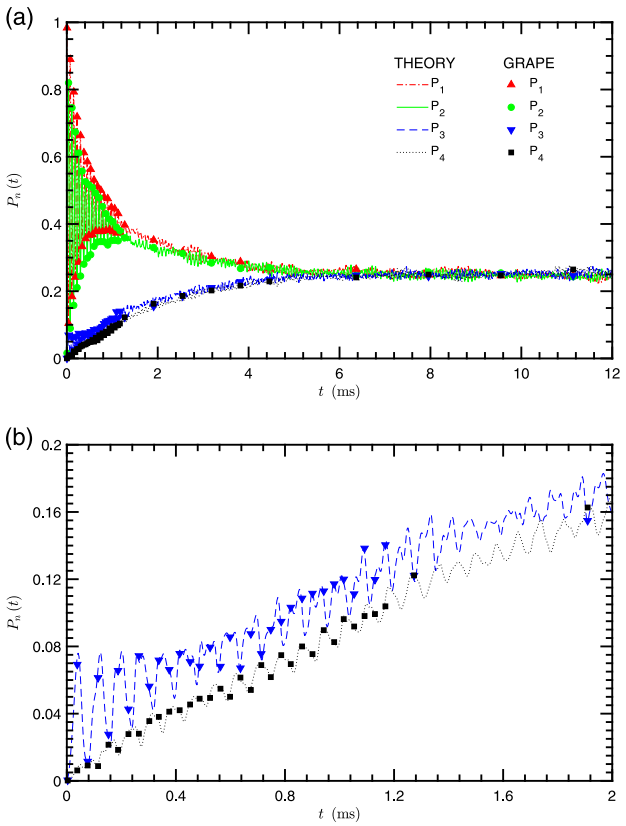

Fig. 5 The long-lasting electronic coherence due to coupling to a vibrational mode. **a** Long-time quantum dynamics; **b** short-time quantum dynamics to show the prolonged coherence of the two lower levels. The symbols show the GRAPE results and the curves show theoretical simulations. The number of realizations in each ensemble is $M = 500$

DISCUSSION

Note that the proof-of-concept NMR experiment presented in this work goes beyond reproducing the HEOM results. To faithfully simulate the EET dynamics on a large photosynthetic system, using the HEOM would be computationally unaffordable. In addition, the HEOM[11,14] is known to encounter difficulties when the spectral density is not in a simple Drude–Lorentz form. As shown in the Supplementary Information, the computational cost of HEOM scales exponentially with the system size and the number of exponentials in the bath correlation function.[11,14] Our NMR simulations do *not* have such shortcomings, as it scales polynomially with respect to the system size.[30,31] Moreover, the quantum simulation algorithm also scales more favorably in terms of the number of exponentials in the bath correlation function. Notice that our simulation proposal is designed for a Gaussian bath. Interestingly, a recently-developed stochastic Liouville equation approach[32] can effectively handle open-system dynamics for spin and fermion bath. In the future it might be beneficial to generalize our approach to handle non-Gaussian baths. With our current approach, in principle, a photosynthetic system with ~100 sites (e.g., the PSI complex) requires a 7-qubit quantum simulator. This means that the coherent EET dynamics of a full functional biological unit for photosynthesis (e.g., the PSII supercomplex that contains ~300 sites) can be faithfully simulated by a 9-qubit NMR quantum computer. Recently, the quantum control on 12 qubits has been successfully demonstrated on an NMR system,[31] where the shortest T_2^* is 150 ms. In natural photosynthetic complexes, the energy transfer is completed within 50 ps. For the scaling factor in our proposal, it corresponds to 7.5 ms, which is smaller than T_2^* by one order of magnitude. Therefore, it is reasonable to simulate the coherent energy transfer within the intrinsic decoherence time of NMR systems. Thus, we believe that NMR quantum simulation has the potential to help clarify the mysteries of light harvesting in natural photosynthesis. In this regard, other approaches, which do not take advantage of this scaling provided by encoding multiple sites into a single qubit,[33] currently lack the required size to simulate such large photosynthetic systems, and thus may also benefit from the approach we develop here.

On the other hand, in natural photosynthetic complexes, the energy is transferred from the outer antenna to the reaction center. In principle, the excitation depletion at the reaction center could be simulated in the NMR platform by coupling auxiliary spins to the energy sink site to remove the population, which is similar to introducing an amplitude damping error in the simulations.[34] In order to prevent the back transfer of energy, there is a large energy gap between the lowest eigenstate of the outer antenna and the reaction center. Thus, the transfer rate from the lowest-energy state to the reaction center is much smaller than the transfer rate within the outer antenna. It is reasonable to simulate the energy transfer without the reaction center.[35] In our theoretical exploration,[13] we investigate the geometrical effects on the energy transfer. In another exploration[36], it was shown that tuning the phases of the inter-molecular couplings can further optimize the energy-transfer efficiency. In future work, it might be interesting to investigate the effect of the couplings' phases on the NMR quantum simulation.

In this paper, the photosynthetic energy transfer is experimentally simulated using NMR. As a prototype, a two-qubit NMR system is utilized to demonstrate both: coherent oscillations in the short-time regime and steady-state thermalization for long times. By using the GRAPE technique, an arbitrary photosynthetic system can be faithfully mapped to the NMR system. Moreover, the effect of the environment on EET can be effectively mimicked by a set of well-designed pulses, which act as a classical pure-dephasing noise. The quantum simulation of photosynthetic energy transfer in NMR would facilitate the investigation of quantum coherent effects on the EET and provide clearer design principles for artificial light-harvesting devices together with structured baths.[13,37]

It was experimentally verified in circuit QED[33] that a structured bath can optimize the energy transfer in EET.[37] Vibrationally assisted energy transfer was demonstrated in a trapped-ion quantum simulator.[38] In both cases, the physical setups therein showed their potential to verify the design principles in optimal photosynthetic light harvesting. However, here we showed that we can use NMR and bath-engineering techniques to efficiently mimic exactly photosynthetic light harvesting in large systems with arbitrary system structure. On the other hand, with our current approach, the simulation may not capture quantum features of the system–environment interaction that arises at stronger couplings and lower temperatures. Capturing such correlations by encoding them in ancillary qubits[39] is a potentially rich avenue for future explorations.

METHODS

Physical parameters

The Hamiltonian $H_{\rm NMR}$ implemented in our NMR simulations is the same as the photosynthetic Hamiltonian $H_{\rm EET}$, but with the unit $\rm cm^{-1}$ divided by $3\times10^4/\pi$. The diagonal terms are

$$H_{\rm NMR}^{11} = 2\pi\times 650\,{\rm kHz}, H_{\rm NMR}^{22} = 2\pi\times 645\,{\rm kHz},$$
$$H_{\rm NMR}^{33} = 2\pi\times 615\,{\rm kHz}, H_{\rm NMR}^{44} = 2\pi\times 610\,{\rm kHz}.$$

The inter-level couplings are: the nearest neighboring couplings

$$H_{\mathrm{NMR}}^{12} = H_{\mathrm{NMR}}^{34} = 2\pi \times 6.3040\,\mathrm{kHz},$$
$$H_{\mathrm{NMR}}^{23} = 2\pi \times 6.5950\,\mathrm{kHz};$$

the next-nearest-neighboring couplings

$$H_{\mathrm{NMR}}^{13} = H_{\mathrm{NMR}}^{24} = 2\pi \times 0.8059\,\mathrm{kHz};$$

and the coupling between the two ends

$$H_{\mathrm{NMR}}^{14} = 2\pi \times 0.2370\,\mathrm{kHz}.$$

The temperature of the photosynthetic energy transfer and NMR experiment are respectively $T_{\mathrm{EET}} = 3 \times 10^4$ K and $T_{\mathrm{NMR}} = 5 \times 10^{-5}$ K. The reorganization energy of the bath is $\lambda_{\mathrm{EET}} = 0.2\,\mathrm{cm}^{-1}$. The cutoff frequency of the bath is $\gamma_{\mathrm{EET}} = 900\,\mathrm{cm}^{-1}$.

Both the Hamiltonian and bath parameters for NMR experiment are those for the photosynthetic energy transfer which are scaled down by a factor of $3 \times 10^8/\pi$.

Initialization

Starting from the thermal-equilibrium state, we prepare a pseudo-pure state[40,41] using the spatial-average technique.[41]

Measurement

The goal is to acquire probability distributions of four states $|00\rangle$, $|01\rangle$, $|10\rangle$, and $|11\rangle$ after the pulse sequences that we designed are implemented on the two-qubit NMR system, namely, four diagonal values of the final density matrix. The density matrices of the output states are reconstructed completely via quantum state tomography.[42] Therefore, the density matrix of the system can be estimated from ensemble averages of a set of observables. For the one-qubit system, the observable set is $\{\sigma_i\}$ ($i = 0, 1, 2, 3$). Here, $\sigma_0 = I$, $\sigma_1 = \sigma_x$, $\sigma_2 = \sigma_y$, $\sigma_3 = \sigma_z$. For the two-qubit system, the observable set is $\{\sigma_i \otimes \sigma_j\}$ ($i, j = 0, 1, 2, 3$). In our experiments, the complete density matrix tomography is not necessary. All we need is to perform two experiments in which the reading-out pulses $\exp(-i\pi\sigma_y/4) \otimes I$ and $I \otimes \exp(-i\pi\sigma_y/4)$ are respectively implemented on the final states of ^{1}H and ^{13}C. The symbols in Fig. 3 are obtained by averaging over $M = 150$ random realizations.

Ramsey spectroscopy

In our experiments, we perform Ramsey spectroscopy for a single qubit subject to Drude–Lorentz noise. In particular, the experiment is divided into three steps:

(1) Preparing the state $|0\rangle$ and rotating it to the xy plane by a $\pi/2$ pulse along the x-axis.
(2) Free evolution while adding the Drude–Lorentz noise.
(3) Applying a reverse $\pi/2$ pulse and measuring the population of the state $|0\rangle$.

We observe that the decay time constant of the population of the state $|0\rangle$ is significantly reduced in the presence of the Drude–Lorentz noise, as shown in Fig. 2. Ramsey fringes are a fit to a cosine with a simple exponential decay envelope. The result by the HEOM theory (blue curve in Fig. 2) is consistent with that in experiments (red dots in Fig. 2). In other words, we demonstrate that $\chi(t) = \mathrm{Re}[g(t)]$.

Vibrational mode

In photosynthetic energy transfer, the coupling to a vibrational mode is described by $\sum_i g_{iv}|i\rangle\langle i|\left(a_{iv}^{\dagger} + a_{iv}\right)$. In order to simulate the underdamped vibrational mode, we can supplement an additional term into Eq. (7), i.e., $aF(v)\sin(\omega_{\mathrm{NMR}}^{v}t)$. Here we choose $\omega_{\mathrm{NMR}}^{v} = 2\pi \times 12.5$ kHz and $aF(v) = \sqrt{0.1 \times \omega_{\mathrm{NMR}}^{v}}$. Since there is no random phase associated with this modulation, i.e., $\psi_v = 0$, each realization will be driven uniformly. Because we set the vibrational mode to be closely-resonant with the two lower exciton states, i.e.,

$$\Delta E_{\mathrm{EET}}^{34} = E_{\mathrm{EET}}^{3} - E_{\mathrm{EET}}^{4} = 251\,\mathrm{cm}^{-1},$$
$$\omega_{\mathrm{EET}}^{v} = 250\,\mathrm{cm}^{-1}$$

and the Huang–Rhys factor $(g_{iv}/\omega_{\mathrm{EET}}^{v})^2 = 0.1$, the long-lived coherence observed in experiments can be effectively simulated, as shown in Fig. 5.

DATA AVAILABILITY

The data that support the findings of this study are available from the corresponding author upon reasonable request.

ACKNOWLEDGEMENTS

We thank Xing-Long Zhen and Ke-Ren Li for discussions. G.L.L. was supported by National Natural Science Foundation of China under Grant Nos. 11175094 and 91221205, and the National Basic Research Program of China under Grant No. 2015CB921001. F.G.D. was supported by the National Natural Science Foundation of China under Grant Nos. 11474026 and 11674033. F.N. was supported in part by the MURI Center for Dynamic Magneto-Optics via the Air Force Office of Scientific Research (AFOSR) (FA9550-14-1-0040), Army Research Office (ARO) (Grant No. 73315PH), Asian Office of Aerospace Research and Development (AOARD) (Grant No. FA2386-18-1-4045), Japan Science and Technology Agency (JST) (the ImPACT program and CREST Grant No. JPMJCR1676), Japan Society for the Promotion of Science (JSPS) (JSPS-RFBR Grant No. 17-52-50023), RIKEN-AIST Challenge Research Fund, and the John Templeton Foundation. Q.A. was supported by the National Natural Science Foundation of China under Grant No. 11505007. This work was supported in part by the Beijing Advanced Innovation Center for Future Chip (ICFC).

AUTHOR CONTRIBUTIONS

All work was carried out under the supervision of G.L.L., F.G.D., Y.C.C., and F.N. B.X.W. and T.X. performed the experiments. Y.C.C., B.X.W., Q.A., M.J.T., and N.L. analyzed the experimental data. M.J.T., Q.A., and N.L. wrote the HEOM simulation code and performed the numerical simulation. Y.C.C. and Q.A. contributed the theory. All authors contributed to writing the manuscript.

ADDITIONAL INFORMATION

Supplementary information accompanies the paper on the *npj Quantum Information* website (https://doi.org/10.1038/s41534-018-0102-2).

Competing interests: The authors declare no competing interests.

Publisher's note: Springer Nature remains neutral with regard to jurisdictional claims in published maps and institutional affiliations.

REFERENCES

1. Cheng, Y.-C. & Fleming, G. R. Dynamics of light harvesting in photosynthesis. *Annu. Rev. Phys. Chem.* **60**, 241–262 (2009).
2. Romero, E., Novoderezhkin, V. I. & van Grondelle, R. Quantum design of photosynthesis for bio-inspired solar-energy conversion. *Nature* **543**, 647–656 (2017).
3. Scholes, G. D. et al. Using coherence to enhance function in chemical and biophysical systems. *Nature* **543**, 647–656 (2017).
4. Lambert, N., Chen, Y.-N., Cheng, Y.-C., Chen, G.-Y. & Nori, F. Quantum biology. *Nat. Phys.* **9**, 10–18 (2013).
5. Engel, G. S. et al. Evidence for wavelike energy transfer through quantum coherence in photosynthetic systems. *Nature* **4**, 782–786 (2007).
6. Chin, A. W. et al. The role of non-equilibrium vibrational structures in electronic coherence and recoherence in pigment–protein complexes. *Nat. Phys.* **9**, 1–6 (2013).
7. Collini, E. et al. Coherently wired light-harvesting in photosynthetic marine algae at ambient temperature. *Nature* **463**, 644–647 (2010).
8. Hildner, R., Brinks, D., Nieder, J. B., Cogdell, R. J. & van Hulst, N. F. Quantum coherent energy transfer over varying pathways in single light-harvesting complexes. *Science* **340**, 1448–1451 (2013).
9. Dong, H., Xu, D. Z., Huang, J.-F. & Sun, C.-P. Coherent excitation transfer via the dark-state channel in a bionic system. *Light Sci. Appl.* **1**, e2 (2012).
10. Xu, L., Gong, Z. R., Tao, M. J. & Ai, Q. Artificial light harvesting by dimerized Möbius ring. *Phys. Rev. E* **97**, 042124 (2018).
11. Ishizaki, A. & Fleming, G. R. Theoretical examination of quantum coherence in a photosynthetic system at physiological temperature. *Proc. Natl. Acad. Sci. U.S.A.* **106**, 17255–17260 (2009).
12. Ai, Q., Fan, Y.-J., Jin, B.-Y. & Cheng, Y.-C. An efficient quantum jump method for coherent energy transfer dynamics in photosynthetic systems under the influence of laser fields. *New J. Phys.* **16**, 053033 (2014).
13. Ai, Q., Yen, T.-C., Jin, B.-Y. & Cheng, Y.-C. Clustered geometries exploiting quantum coherence effects for efficient energy transfer in light harvesting. *J. Phys. Chem. Lett.* **4**, 2577–2584 (2013).

14. Tanimura, Y. Stochastic Liouville, Langevin, Fokker–Planck, and master equation approaches to quantum dissipative systems. *J. Phys. Soc. Jpn.* **75**, 082001 (2006).
15. Li, C. M., Lambert, N., Chen, Y. N., Chen, G. Y. & Nori, F. Witnessing quantum coherence: from solid-state to biological systems. *Sci. Rep.* **2**, 885 (2012).
16. Tao, M.-J., Ai, Q., Deng, F.-G. & Cheng, Y.-C. Proposal for probing energy transfer pathway by single molecule pump–dump experiment. *Sci. Rep.* **6**, 27535 (2016).
17. Buluta, I. & Nori, F. Quantum simulators. *Science* **326**, 108–111 (2009).
18. Georgescu, I., Ashhab, S. & Nori, F. Quantum simulation. *Rev. Mod. Phys.* **86**, 153–185 (2014).
19. Buluta, I., Ashhab, S. & Nori, F. Natural and artificial atoms for quantum computation. *Rep. Prog. Phys.* **74**, 104401 (2011).
20. Soare, A. et al. Experimental noise filtering by quantum control. *Nat. Phys.* **10**, 825–829 (2014).
21. Zhen, X.-L., Zhang, F.-H., Feng, G. R., Li, H. & Long, G.-L. Optimal experimental dynamical decoupling of both longitudinal and transverse relaxations. *Phys. Rev. A* **93**, 022304 (2016).
22. Luo, Z. H. et al. Experimentally probing topological order and its breakdown through modular matrices. *Nat. Phys.* **14**, 160–165 (2018).
23. Feng, G. R., Xu, G. F. & Long, G. L. Experimental realization of nonadiabatic holonomic quantum computation. *Phys. Rev. Lett.* **110**, 190501 (2013).
24. Chuang, I. L., Vandersypen, L. M. K., Zhou, X. L., Leung, D. W. & Lloyd, S. Experimental realization of a quantum algorithm. *Nature* **393**, 143–146 (1998).
25. Khaneja, N., Reiss, T., Kehlet, C. & Schulte-Herbrüggen, T. Optimal control of coupled spin dynamics: design of NMR pulse sequences by gradient ascent algorithms. *J. Magn. Reson.* **172**, 296–305 (2005).
26. Zhang, J. F., Wei, T.-C. & Laflamme, R. Experimental quantum simulation of entanglement in many-body systems. *Phys. Rev. Lett.* **107**, 010501 (2011).
27. Peng, X. H. et al. Experimental implementation of adiabatic passage between different topological orders. *Phys. Rev. Lett.* **113**, 080404 (2014).
28. Santamore, D. H., Lambert, N. & Nori, F. Vibrationally mediated transport in molecular transistors. *Phys. Rev. B* **87**, 075422 (2013).
29. Wertnik, M., Chin, A. W., Nori, F. & Lambert, N. Optimizing co-operative multi-environment dynamics in a dark-state-enhanced photosynthetic heat engine. *J. Chem. Phys.* **149**, 084112 (2018).
30. Li, J., Yang, X. D., Peng, X. H. & Sun, C.-P. Hybrid quantum-classical approach to quantum optimal control. *Phys. Rev. Lett.* **118**, 150503 (2017).
31. Lu, D. W. et al. Enhancing quantum control by bootstrapping a quantum processor of 12 qubits. *npj Quantum Inf.* **3**, 45 (2017).
32. Hsieh, C.-Y. & Cao, J. S. A unified stochastic formulation of dissipative quantum dynamics. I. Generalized hierarchical equations. *J. Chem. Phys.* **148**, 014103 (2018).
33. Potŏnik, A. et al. Studying light-harvesting models with superconducting circuits. *Nat. Commun.* **9**, 904 (2018).
34. Nielsen, M. & Chuang, I. *Quantum Computation and Quantum Information*. (University Press, Cambridge, 2000).
35. Moix, J. M., Zhao, Y. & Cao, J. S. Equilibrium-reduced density matrix formulation: Influence of noise, disorder, and temperature on localization in excitonic systems. *Phys. Rev. B* **85**, 115412 (2012).
36. Cao, J. S. & Silbey, R. J. Optimization of exciton trapping in energy transfer processes. *J. Phys. Chem. A* **113**, 13825–13838 (2009).
37. del Rey, M., Chin, A. W., Huelga, S. F. & Plenio, M. B. Exploiting structured environments for efficient energy transfer: the phonon antenna mechanism. *J. Phys. Chem. Lett.* **4**, 903–907 (2013).
38. Gorman, D. J. et al. Engineering vibrationally assisted energy transfer in a trapped-ion quantum simulator. *Phys. Rev. X* **8**, 011038 (2018).
39. Chen, H.-B., Gneiting, C., Lo, P.-Y., Chen, Y.-N. & Nori, F. Simulating open quantum systems with Hamiltonian ensembles and the nonclassicality of the dynamics. *Phys. Rev. Lett.* **120**, 030403 (2018).
40. Gershenfeld, N. A. & Chuang, I. L. Bulk spin-resonance quantum computation. *Science* **275**, 350–356 (1997).
41. Cory, D. G., Fahmy, A. F. & Havel, T. F. Ensemble quantum computing by NMR spectroscopy. *Proc. Natl. Acad. Sci. U.S.A.* **94**, 1634–1639 (1997).
42. Xin, T. et al. Quantum state tomography via reduced density matrices. *Phys. Rev. Lett.* **118**, 020401 (2017).